PHYSICAL REVIEW B **97**, 241110(R) (2018)

Rapid Communications

Robust non-Abelian spin liquid and a possible intermediate phase in the antiferromagnetic Kitaev model with magnetic field

Zheng Zhu,[1] Itamar Kimchi,[1] D. N. Sheng,[2] and Liang Fu[1]

[1]*Department of Physics, Massachusetts Institute of Technology, Cambridge, Massachusetts 02139, USA*

[2]*Department of Physics and Astronomy, California State University, Northridge, California 91330, USA*

(Received 30 October 2017; revised manuscript received 13 April 2018; published 15 June 2018)

We investigate the non-Abelian topological chiral spin-liquid phase in the two-dimensional Kitaev honeycomb model subject to a magnetic field. By combining density matrix renormalization group and exact diagonalization we study the energy spectra, entanglement, topological degeneracy, and expectation values of Wilson loop operators, allowing for a robust characterization. While the ferromagnetic Kitaev spin liquid is already destroyed by a weak magnetic field with Zeeman energy $H_*^{\mathrm{FM}} \approx 0.02$, the antiferromagnetic (AFM) spin liquid remains robust up to a magnetic field that is an order of magnitude larger, $H_*^{\mathrm{AFM}} \approx 0.2$. Interestingly, for larger fields $H_*^{\mathrm{AFM}} < H < H_{**}^{\mathrm{AFM}}$, an intermediate gapless phase is observed, before a second transition to the high-field partially polarized paramagnet. We attribute this rich phase diagram, and the remarkable stability of the chiral topological phase in the AFM Kitaev model, to the interplay of strong spin-orbit coupling and frustration enhanced by the magnetic field. Our findings suggest relevance to recent experiments on $RuCl_3$ under magnetic fields.

DOI: 10.1103/PhysRevB.97.241110

Introduction. The search for highly entangled quantum states of matter such as quantum spin liquids (QSLs) has intensified in recent years [1–4]. The peculiarity of QSLs lies not only in the absence of magnetic long-range order even at zero temperature, but, more importantly, in exhibiting fractionalized excitations and topological ground-state degeneracy. Among various theoretically proposed QSLs, a remarkable example is the Kitaev model of spins with nearest-neighbor interactions on the two-dimensional (2D) honeycomb lattice [5]. This model is solved exactly by mapping it into a model of Majorana fermions coupled to an emergent static $\mathbb{Z}_2$ gauge field. The ground state is either a gapless spin liquid or, with weak time-reversal breaking, a gapped spin-liquid phase. The latter harbors a non-Abelian anyon known as an Ising anyon, a descendant of vortices in two-dimensional $p+ip$ superconductors [6]. The exact solution of the apparently simple Kitaev model has motivated a search for the physical realization of non-Abelian QSLs [7–9].

The highly anisotropic and spatially dependent spin interaction in the Kitaev model can conceivably appear in Mott insulators with strong spin-orbit coupling and $j = 1/2$ local moments. In particular, Jackeli and Khaliullin [10] proposed a mechanism for the Kitaev interaction in transition-metal oxides with edge-sharing oxygen octahedra. By now, in addition to various three-dimensional compounds [11–13], a variety of two-dimensional layered honeycomb lattice magnets [14] have been discovered, including Na_2IrO_3 [15–17], α-Li_2IrO_3 [16,17], a hydrated variant $H_3LiIr_2O_6$ [18], and $RuCl_3$ [19].

Aside from the spin-liquid candidates $Na_4Ir_3O_8$ (hyperkagome [11,20]) and $H_3LiIr_2O_6$ (honeycomb [18]), these compounds are magnetically ordered at sufficiently low temperatures, indicating the presence of additional spin interactions beyond the Kitaev model. Nonetheless, various experimental and theoretical works suggest the magnetic ordered states are proximate to a spin-liquid phase [9,21–32]. To understand the nature of quantum phases realized in materials, it is helpful to compare the experimental findings with the expected signatures of perturbed Kitaev Hamiltonians. However, even with the large body of available experimental data, the sign of the Kitaev interaction in the honeycomb magnets remains an open question [25–31,33–43]. In models with strong spin-orbit coupling, the Curie-Weiss temperature may not reflect the dominant interaction due to cancellation among the various spin-orbit-coupled exchanges; for instance, T_{CW} may even vanish [44]. Interestingly, for $RuCl_3$, it has recently been argued that natural models with nearest-neighbor exchanges involve a strong Γ exchange or have a dominant, likely *antiferromagnetic*, Kitaev exchange [26,27,45].

For the pure Kitaev model, the different signs of the Kitaev exchange are related by a sublattice-dependent transformation, leading to an identical energy spectrum. However, under an external magnetic field, ferromagnetic (FM) and antiferromagnetic (AFM) Kitaev models are expected to behave differently. Previous theoretical studies mainly focused on the FM Kitaev model, and found that the non-Abelian spin-liquid phase only survives up to a very small magnetic field, $H_*^{\mathrm{FM}} \approx 0.02$ by Jiang *et al.* [46]. To our knowledge, except semiclassically [47], the AFM Kitaev model in a magnetic field has not yet been studied.

In this Rapid Communication, we study the AFM Kitaev model in a magnetic field by performing extensive exact diagonalization (ED) and density matrix renormalization group (DMRG) simulations. The energy spectra, the expectation value of the Wilson loop operator, and the ground-state degeneracy as a function of the magnetic field are computed and compared with exact analytical results at zero field. We find the presence of the non-Abelian QSL phase in the AFM Kitaev model over a wide range of magnetic field up to $H_*^{\mathrm{AFM}} \approx 0.2$, an order of magnitude larger than that of the FM Kitaev model. Moreover, before a second transition at $H_{**}^{\mathrm{AFM}} \approx 0.36$ to

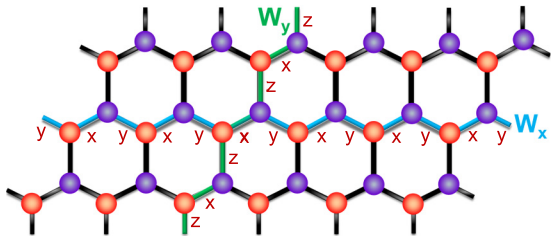

FIG. 1. The honeycomb lattice and Wilson loop operators. The honeycomb lattice is spanned by unit vectors (1,0) and $(1/2,\sqrt{3}/2)$ with a lattice size $N = L_x \times L_y \times 2$. Green and blue loops denote Wilson loop operators along the vertical and horizontal periodic boundary conditions on the torus, respectively.

the high-field partially polarized paramagnet, an intermediate gapless phase is observed for fields $H_*^{\mathrm{AFM}} < H < H_{**}^{\mathrm{AFM}}$.

Model and method. We consider the Kitaev honeycomb model subject to an external magnetic field $\mathbf{H}$ along the $\langle 111 \rangle$ direction. The Hamiltonian is given by

$$H = \sum_{\langle i,j \rangle} K_\gamma S_i^\gamma S_j^\gamma - \sum_i \mathbf{H} \cdot \mathbf{S}_i. \tag{1}$$

Here, $\gamma = x,y,z$ denote the three distinct nearest-neighbor links $\langle i,j \rangle$ of the hexagonal lattice (see Fig. 1), and S^γ represents effective spin-1/2 degrees of freedom sitting on each vertex and interacting via exchange K_γ. The ground state at $\mathbf{H} = \mathbf{0}$ corresponds to the Kitaev limit, which exhibits two kinds of QSLs depending on the relative coupling strength. When one of the three coupling K_γ is much larger than the others, the system is a gapped $\mathbb{Z}_2$ spin liquid with Abelian excitations, while around the isotropic point of equal couplings, the system is a gapless spin liquid [5]. The latter can turn into a non-Abelian topological phase under time-reversal symmetry breaking perturbations [5], e.g., by adding a three-spin chirality term [48], or by applying an external magnetic field [5], or by decorating the honeycomb lattice [49].

We use both exact diagonalization (ED) and density matrix renormalization group (DMRG) to study the Hamiltonian (1) with isotropic coupling $K_\gamma \equiv K$, as a function of an external magnetic field $\mathbf{H}$. We compare the phase diagrams with AFM ($K > 0$) and FM ($K < 0$) Kitaev couplings.

In the present calculation, we consider a system of size $N = L_x \times L_y \times 2$ (see Fig. 1), where L_x and L_y represent the number of unit cells along the x and y directions, respectively. Our present DMRG calculations keep enough states to ensure the truncation error of the order of or smaller than 10^{-9} and perform DMRG sweeps until the measured quantities are converged.

Non-Abelian topological phase. We first compute the energy spectra of the model Hamiltonian Eq. (1) as a function of the magnetic field. Figure 2 shows the low-energy spectra in different momentum sectors for a system size $N = 4 \times 3 \times 2$ on the torus, with antiferromagnetic ($K = +1$) or ferromagnetic ($K = -1$) Kitaev couplings. For the antiferromagnetic case, we find the two lowest-energy states in the $(\pi,0)$ and (0,0) momentum sectors, which are separated from the higher-energy states by a finite gap for a range of magnetic field $0 \leqslant H_{111} \lesssim 0.2$. In contrast, in the case with ferromagnetic Kitaev coupling, the spectra shown in Fig. 2(b) indicate that the topological phase only survives in a much smaller regime at $H_{111} \lesssim 0.02$. Meanwhile, while naively one would expect a transition directly to the partially polarized phase (which is smoothly connected to the fully polarized $H_{111} = \infty$ limit), as is indeed seen in the FM Kitaev model [see Figs. 2(b), 2(e) and 2(f)], here for the AFM Kitaev model, as shown in Figs. 2(a), 2(e) and 2(f), an intermediate gapless phase (discussed further below) is observed at $H_*^{\mathrm{AFM}} < H < H_{**}^{\mathrm{AFM}}$ before a transition to the polarized paramagnet at $H_{**}^{\mathrm{AFM}} \approx 0.36$. In both AFM and FM cases, the critical field is also identified by sharp peaks in the second-order derivative of the ground-state energy, or equivalently the magnetic susceptibility [see Fig. 2(f)]. Similarly to the FM case [46], the field-driven phase transitions in the AFM case might be continuous or weakly first order.

We now demonstrate the topological nature of the two lowest-energy states below the critical field H_*. First, we note that the Kitaev model at zero field with periodic boundary conditions has topological ground-state degeneracy in two dimensions. Different ground states are characterized by two Wilson loop operators W_y and W_x associated with noncontractible loops along the y and x directions, respectively. As illustrated in Fig. 1, the definitions of W_y and W_x are given by

$$W_y = -\left\langle \prod_{i=1}^{2L_y} \sigma_i^y \right\rangle, \quad W_x = -\left\langle \prod_{i=1}^{2L_x} \sigma_i^z \right\rangle, \tag{2}$$

where σ^y and σ^z are Pauli matrices [50], i.e., twice the spin-1/2 operators. The loops along the y direction only cover $\gamma = x,z$ links while the loops along the x direction only cover the $\gamma = x,y$ links. It is straightforward to verify that these Wilson loop operators commute with each other and also with the Hamiltonian in the Kitaev limit. Each operator squares to identity, hence its eigenvalue is either $+1$ or -1. The ± 1 eigenvalue of Wilson loop operator corresponds to the Z_2 fluxes or equivalently the periodic/antiperiodic boundary conditions for the emergent Majorana fermions.

The expectation values of Wilson loop operators $W_{x,y}$ are measured for these two lowest-energy states in the model (1). As shown in Figs. 2(c) and 2(d), these Wilson loop operators take exact quantized values in the Kitaev limit and nearly quantized values for a finite range of magnetic fields below the critical value. This indicates that the emergent $\mathbb{Z}_2$ gauge theory remains a good description of the perturbed Kitaev model away from the static limit. Importantly, below the critical field, the two lowest-energy states have nearly the same value of $W_y \simeq -1$ but distinct values of W_x, with $W_x \simeq +1$ for the state in momentum $(\pi,0)$ sector and $W_x \simeq -1$ for the state in the (0,0) sector, as shown in the inset of Fig. 2(c). These results are fully consistent with our expectation that the degeneracy between different topological sectors of the Kitaev phase in the thermodynamic limit is split by the finite-size effect in a quasi-one-dimensional geometry. For a three-leg system studied in this work, the splitting between the $W_y = 1$ and $W_y = -1$ sectors is strong enough that the two lowest-energy states both have $W_y \simeq -1$. As we shall show below, these two lowest-energy states become degenerate as L_x increases. Their many-body momenta $k_x = 0$ and π indicate that as a one-dimensional (1D) system, the three-leg AFM Kitaev model spontaneously breaks translational symmetry breaking and doubles the unit cell in the thermodynamic limit. This

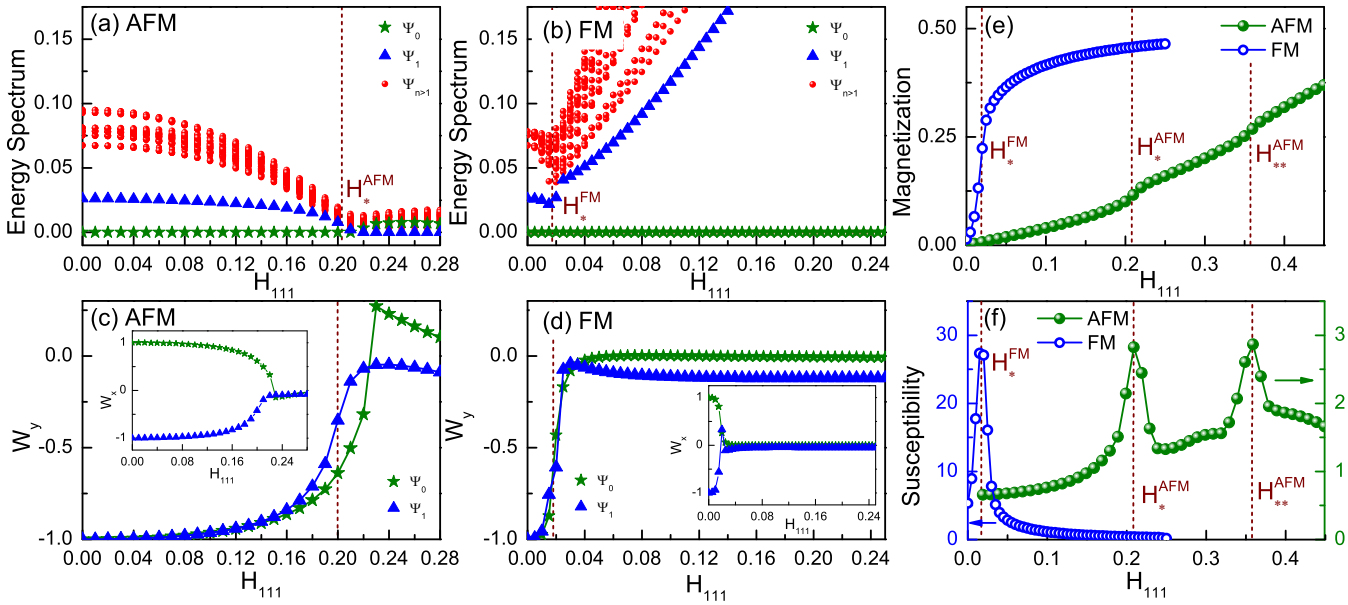

FIG. 2. (a), (b) For the (a) AFM and (b) FM Kitaev models in a magnetic field, the pair of topological ground states (approximately degenerate on this $N = 4\times3\times2$ torus) are separated from higher-energy states by an energy gap, within the topological phase $H < H_*$, where $H_*^{\rm AFM} \approx 0.2$ and $H_*^{\rm FM} \approx 0.02$. (c), (d) Wilson loop operators W_y (main panel) and W_x (inset) for the two lowest-energy states, for (c) AFM and (d) FM models. The two states have $W_y = -1$ but are distinguished by $W_x = \pm 1$. (e) The magnetization curves show the transitions and the stark difference between the AFM and FM models. (f) The second-order derivative of ground-state energy with respect to field, or equivalently the magnetic susceptibility: Note the difference in magnitudes between AFM and FM models. In the AFM case, the transition to the polarized high-field phase is achieved only at a second peak with $H_{**} \approx 0.36$.

is analogous to the charge-density-wave states obtained by placing $\nu = 1/3$ fractional quantum Hall states on a thin torus.

The expectation values of Wilson loop operators decay rapidly near the critical field and become negligible above the critical field. The near quantization of Wilson loop operators (and lack thereof) provides more strong evidence for the topological (nontopological) nature of the phases before (after) the phase transition.

For the AFM Kitaev model, we further use DMRG to calculate the ground-state degeneracy at $H_{111} \lesssim 0.2$ for large L_x to confirm its topological nature. In Fig. 2(a), we find a small energy split between the two lowest-energy states. To confirm these two states are exactly degenerate states in the thermodynamic limit, we perform a DMRG calculation on the torus by targeting the three lowest-energy states with increasing L_x. As shown in Fig. 3(a), we find that the energy difference between the two lowest states $E_1 - E_0$ becomes vanishingly small when the system length $L_x \gtrsim 8$, while the two lowest states are separated from the higher-energy states by a finite gap indicated by $E_2 - E_0$ [see Fig. 3(a)]. Based on these calculations, the twofold ground-state degeneracy of such a topological phase is identified. Meanwhile, we also checked the Wilson loop operator W_y for different $L_y = 3$ system sizes by DMRG, as shown in Fig. 3(b), and we find the topological phase to be very robust and independent of system length.

The gapped feature of the topological phase can also be confirmed by the von Neumann entanglement entropy $S_{\rm VN}$ defined by $S_{\rm VN} = -{\rm Tr}(\rho_A \ln \rho_A)$, where ρ_A is the reduced density matrix of part A for the bipartition of the system into A and B, and ρ_A is obtained by tracing out the degrees of freedom of the B part. Here, we consider the cut parallel to the y direction and measure the value of $S_{\rm VN}$ for each cut at L_A. For the gapped state, the von Neumann entropy should be independent of the positions of each cut and display flat behavior. As shown in Fig. 4(b), we calculate a long cylinder by DMRG and find the flat $S_{\rm VN}$ as a function of L_A, implying the existence of a well-defined gap in the topological phase. All of these confirm the stability of the topological phase.

In the absence of magnetic field, the Kitaev model is exactly solvable in terms of static fluxes and Majorana fermions [5]. We also analyze the exact solution on finite systems as well as infinite ladders. In each topological sector defined by a particular set of values of the Wilson loop operators, the ground-state

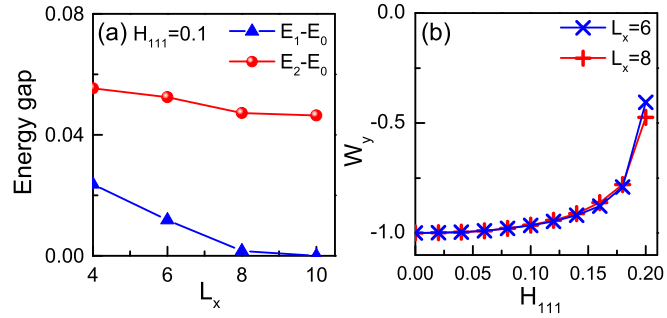

FIG. 3. (a) The DMRG calculation of the three lowest-energy states as a function of L_x at $H_{111} = 0.1$ on the torus. The energy difference between the two lowest-energy states becomes vanishingly small with increasing system size while they are separated from the higher-energy sectors by a finite gap. (b) The DMRG results of the Wilson loop operator W_y on the torus for the antiferromagnetic (AFM) Kitaev model with $L_x = 6,8$.

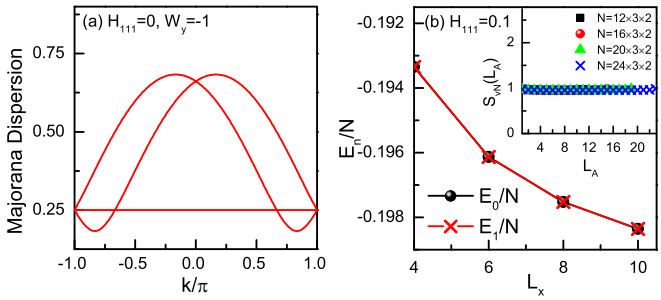

FIG. 4. (a) Majorana dispersions on infinite ladders ($L_y = 3$) for the $W_y = -1$ sector at $H_{111} = 0$, which show a finite gap and a quantized value of Wilson loop operators. These are consistent with the numerics for finite fields (see main text). (b) The energy density of two degenerate states on cylinders at $H_{111} = 0.1$; the inset shows the von Neumann entanglement entropy for long cylinders, where the flat feature indicates the existence of the finite gap.

energy is simply given by the energy of the filled Fermi sea, i.e., the sum of all negative Majorana eigenvalues. Figure 4(a) shows the Majorana dispersion for infinite cylinders in the $W_y = -1$ sector with fixed width $L_y = 3$. We also compared the exact solution on finite-size systems with DMRG and ED results, which are consistent with each other.

Interestingly, the three-leg system with $W_y = -1$ as we identified here is a one-dimensional topological superconductor of Majorana fermions in the thermodynamic limit $L_x \to \infty$. This is shown by computing $\mathrm{sgn}[\mathrm{Pf}[H[0]]\mathrm{Pf}[H[\pi]]]$, i.e., the sign of the product of Pfaffians of the quadratic Majorana Hamiltonian matrices at 1D momenta $k = 0$ and $k = \pi$. We find a negative value for this topological index correspond to a 1D topological superconductor [51]. Therefore, we expect the presence of boundary Majorana zero modes for open boundary conditions in the L_x direction. These boundary zero modes can be regarded as a descendent of non-Abelian anyons in the Kitaev phase in two dimensions, and their presence should be robust against perturbations such as the magnetic field. Indeed, we find the two lowest states are exactly degenerate on cylinders by DMRG, as shown in Fig. 4(b) for $H_{111} = 0.1$, and the twofold degeneracy in the entanglement spectrum on the cylinders, confirming the existence of Majorana zero modes on the boundary.

Discussion and summary. In this Rapid Communication, we report a robust non-Abelian phase in the antiferromagnetic Kitaev model under a magnetic field. Based on extensive DMRG and ED simulations, we identify its topological features by the energy spectra, entanglement, topological degeneracy, and Wilson loop operators. We find that the topological phase in the antiferrmagnetic Kitaev model is much more stable to increasing magnetic field than the one in the ferromagnetic Kitaev model. This can be partially understood from the low-field magnitude of magnetic susceptibility [insets of Figs. 2(a) and 2(b)], which in turn has a simple interpretation. While at zero field the AFM and FM Kitaev models are exactly equivalent by a Majorana sign transformation on one honeycomb sublattice [5], since their spin correlations are identical except opposite in sign, the FM Kitaev model is nearly a ferromagnet, while the AFM model has a similar strong response to a staggered magnetic field but a weak response to a uniform field. This difference between the AFM and FM Kitaev coupling can also be seen approaching from the infinite field limit [47] based on a semiclassical spin-wave analysis. Our findings suggest that, in materials with dominant antiferromagnetic Kitaev interactions, a spin-liquid phase, if present, may be observable under an application of fairly substantial magnetic fields, in contrast to previous expectations.

Moreover, when the gapped chiral topological order is destroyed by the large field in the AFM case, before entering the polarized phase, an intermediate gapless phase is found. Within the intermediate gapless phase of the AFM model, the DMRG algorithm converges to a state exhibiting modulations in spin density around the partially polarized mean (about 10%–20% of full amplitude), which appear to be pinned by the open boundaries (see the Supplemental Material [52] for details). Together with the gapless spectrum [Fig. 2(a)] and the large entanglement, these observations serve as evidence that this gapless phase involves long-range correlations or entanglement, and thus it cannot be captured reliably in the 2D limit. A possible connection to experiments remains an open question.

Acknowledgments. We would like to thank J. Analytis, R. Coldea, and Y. Qi for insightful discussions. Z.Z. and L.F. are supported by the David and Lucile Packard Foundation. I.K. is supported by the MIT Pappalardo Fellowship. D.N.S. is supported by the U.S. Department of Energy, Office of Basic Energy Sciences under Grant No. DE-FG02-06ER46305. Z.Z. used the Extreme Science and Engineering Discovery Environment (XSEDE) to perform part of the simulation, which is supported by National Science Foundation Grant No. ACI-1548562.

[1] X.-G. Wen, *Quantum Field Theory of Many-Body Systems* (Oxford University Press, Oxford, UK, 2004).
[2] P. A. Lee, Science **321**, 1306 (2008).
[3] L. Savary and L. Balents, Rep. Prog. Phys. **80**, 016502 (2017), and references therein; L. Balents, Nature (London) **464**, 199 (2010).
[4] Y. Zhou, K. Kanoda, and T.-K. Ng, Rev. Mod. Phys. **89**, 025003 (2017), and references therein.
[5] A. Kitaev, Ann. Phys. **321**, 2 (2006).
[6] N. Read and D. Green, Phys. Rev. B **61**, 10267 (2000).
[7] J. G. Rau, E. K.-H. Lee, and H.-Y. Kee, Annu. Rev. Condens. Matter Phys. **7**, 195 (2016), and references therein.
[8] S. Trebst, arXiv:1701.07056.
[9] M. Hermanns, I. Kimchi, and J. Knolle, Annu. Rev. Condens. Matter Phys. **9**, 17 (2018), and references therein.
[10] G. Jackeli and G. Khaliullin, Phys. Rev. Lett. **102**, 017205 (2009).
[11] Y. Okamoto, M. Nohara, H. Aruga-Katori, and H. Takagi, Phys. Rev. Lett. **99**, 137207 (2007).
[12] K. A. Modic, T. E. Smidt, I. Kimchi, N. P. Breznay, A. Biffin, S. Choi, R. D. Johnson, R. Coldea, P. Watkins-Curry, G. T. McCandless, J. Y. Chan, F. Gandara, Z. Islam, A. Vishwanath, A. Shekhter, R. D. McDonald, and J. G. Analytis, Nat. Commun. **5**, 4203 (2014).

[13] T. Takayama, A. Kato, R. Dinnebier, J. Nuss, H. Kono, L. S. I. Veiga, G. Fabbris, D. Haskel, and H. Takagi, Phys. Rev. Lett. **114**, 077202 (2015).
[14] J. Chaloupka, G. Jackeli, and G. Khaliullin, Phys. Rev. Lett. **105**, 027204 (2010).
[15] S. K. Choi, R. Coldea, A. N. Kolmogorov, T. Lancaster, I. I. Mazin, S. J. Blundell, P. G. Radaelli, Yogesh Singh, P. Gegenwart, K. R. Choi, S.-W. Cheong, P. J. Baker, C. Stock, and J. Taylor, Phys. Rev. Lett. **108**, 127204 (2012).
[16] Y. Singh and P. Gegenwart, Phys. Rev. B **82**, 064412 (2010).
[17] Y. Singh, S. Manni, J. Reuther, T. Berlijn, R. Thomale, W. Ku, S. Trebst, and P. Gegenwart, Phys. Rev. Lett. **108**, 127203 (2012).
[18] H. Takagi, talk given at the KITP conference on Order, Fluctuations, and Strong Correlations: New Platforms and Developments, June 2017, http://online.kitp.ucsb.edu/online/intertwined_c17/takagi/.
[19] K. W. Plumb, J. P. Clancy, L. J. Sandilands, V. V. Shankar, Y. F. Hu, K. S. Burch, H.-Y. Kee, and Y.-J. Kim, Phys. Rev. B **90**, 041112 (2014).
[20] I. Kimchi and A. Vishwanath, Phys. Rev. B **89**, 014414 (2014).
[21] M. Gohlke, G. Wachtel, Y. Yamaji, F. Pollmann, and Y. B. Kim, Phys. Rev. B **97**, 075126 (2018).
[22] M. Gohlke, R. Verresen, R. Moessner, and F. Pollmann, Phys. Rev. Lett. **119**, 157203 (2017).
[23] V. M. Katukuri, S. Nishimoto, V. Yushankhai, A. Stoyanova, H. Kandpal, S. Choi, R. Coldea, I. Rousochatzakis, L. Hozoi, and J. van den Brink, New J. Phys. **16**, 013056 (2014).
[24] Z. Wang, S. Reschke, D. Hüvonen, S.-H. Do, K.-Y. Choi, M. Gensch, U. Nage, T. Rõõm, and A. Loidl, Phys. Rev. Lett. **119**, 227202 (2017).
[25] S. M. Winter, K. Riedl, D. Kaib, R. Coldea, and R. Valenti, Phys. Rev. Lett. **120**, 077203 (2018).
[26] A. Banerjee, C. A. Bridges, J.-Q. Yan, A. A. Aczel, L. Li, M. B. Stone, G. E. Granroth, M. D. Lumsden, Y. Yiu, J. Knolle, D. L. Kovrizhin, S. Bhattacharjee, R. Moessner, D. A. Tennant, D. G. Mandrus, and S. E. Nagler, Nat. Mater. **15**, 733 (2016).
[27] L. Janssen, E. C. Andrade, and M. Vojta, Phys. Rev. B **96**, 064430 (2017).
[28] A. Banerjee, J. Yan, J. Knolle, C. A. Bridges, M. B. Stone, M. D. Lumsden, D. G. Mandrus, D. A. Tennant, R. Moessner, and S. E. Nagler, Science **356**, 1055 (2017).
[29] A. Banerjee, P. Lampen-Kelley, J. Knolle, C. Balz, A. A. Aczel, B. Winn, Y. Liu, D. Pajerowski, J.-Q. Yan, C. A. Bridges, A. T. Savici, B. C. Chakoumakos, M. D. Lumsden, D. A. Tennant, R. Moessner, D. G. Mandrus, and S. E. Nagler, npj Quantum Mater. **3**, 8 (2018).
[30] A. N. Ponomaryov, E. Schulze, J. Wosnitza, P. Lampen-Kelley, A. Banerjee, J.-Q. Yan, C. A. Bridges, D. G. Mandrus, S. E. Nagler, A. K. Kolezhuk, and S. A. Zvyagin, Phys. Rev. B **96**, 241107 (2017).
[31] A. Little, L. Wu, P. Lampen-Kelley, A. Banerjee, S. Patankar, D. Rees, C. A. Bridges, J.-Q. Yan, D. Mandrus, S. E. Nagler, and J. Orenstein, Phys. Rev. Lett. **119**, 227201 (2017).
[32] X.-Y. Song, Y.-Z. You, and L. Balents, Phys. Rev. Lett. **117**, 037209 (2016).
[33] K. Ran, J. Wang, W. Wang, Z.-Y. Dong, X. Ren, S. Bao, S. Li, Z. Ma, Y. Gan, Y. Zhang, J. T. Park, G. Deng, S. Danilkin, S.-L. Yu, J.-X. Li, and J. Wen, Phys. Rev. Lett. **118**, 107203 (2017).
[34] W. Wang, Z.-Y. Dong, S.-L. Yu, and J.-X. Li, Phys. Rev. B **96**, 115103 (2017).
[35] Y. Sizyuk, P. Wölfle, and N. B. Perkins, Phys. Rev. B **94**, 085109 (2016).
[36] H.-S. Kim and H.-Y. Kee, Phys. Rev. B **93**, 155143 (2016).
[37] J. Chaloupka and G. Khaliullin, Phys. Rev. B **94**, 064435 (2016).
[38] S. M. Winter, Y. Li, H. O. Jeschke, and R. Valenti, Phys. Rev. B **93**, 214431 (2016).
[39] J. Chaloupka and G. Khaliullin, Phys. Rev. B **92**, 024413 (2015).
[40] I. Rousochatzakis, J. Reuther, R. Thomale, S. Rachel, and N. B. Perkins, Phys. Rev. X **5**, 041035 (2015).
[41] H.-S. Kim, V. Vijayshanka, A. Catuneanu, and H.-Y. Kee, Phys. Rev. B **91**, 241110(R) (2015).
[42] J. G. Rau, E. K.-H. Lee, and H. Y. Kee, Phys. Rev. Lett. **112**, 077204 (2014).
[43] Y. Yamaji, Y. Nomura, M. Kurita, R. Arita, and M. Imada, Phys. Rev. Lett. **113**, 107201 (2014).
[44] J. Reuther, R. Thomale, and S. Trebst, Phys. Rev. B **84**, 100406(R) (2011).
[45] J. Chaloupka, G. Jackeli, and G. Khaliullin, Phys. Rev. Lett. **110**, 097204 (2013).
[46] H.-C. Jiang, Z.-C. Gu, X.-L. Qi, and S. Trebst, Phys. Rev. B **83**, 245104 (2011).
[47] L. Janssen, E. C. Andrade, and M. Vojta, Phys. Rev. Lett. **117**, 277202 (2016).
[48] D.-H. Lee, G.-M. Zhang, and T. Xiang, Phys. Rev. Lett. **99**, 196805 (2007).
[49] H. Yao and S. A. Kivelson, Phys. Rev. Lett. **99**, 247203 (2007).
[50] The necessity of the minus sign in these formulas can be seen by considering the Z_2 gauge fields along the path of the Wilson loop traversing the periodic boundary conditions.
[51] A. Kitaev, Phys. Usp. **44**, 131 (2001).
[52] See Supplemental Material at http://link.aps.org/supplemental/10.1103/PhysRevB.97.241110 for more numerical data of the intermediate phase.